SUPPORTING INFORMATION LEGENDS

Figure S1. JAK/STAT and AMPK signaling pathways in ESCs change extensively in response to aging. (A) JAK/STAT and (B) AMPK pathway gene expression perturbations in young vs aged mouse epidermal stem cells from dataset GSE84511. Each node represents a set of genes and the color coding reflects gene expression changes within the node. Wiring diagrams generated using the Pathview and GAGE bioconductor package with 5% FDR (BH).

Figure S2. Recombinant mouse IL-15 treatment reduces hallmarks of senescence in skin without impacting T-cells. (A) Cytochrome c oxidase activity measured on Day 42 intact skin epidermal lysates. n = 4-6 mice per group. (B) Representative immunofluorescent images of epidermal and dermal HMGB1 and Lamin B1 staining of young control (Young PBS), old control (Old PBS) and old rmIL-15 (Old rmIL-15) treated intact skin taken during wound surgery and (C, D) quantification of images from (A). n = 4-8 mice per group. (E) Spleen weights of mice from each treatment group normalized to individual body weights. n = 4-6 mice per group. (F) Representative micrographs of epidermal CD3 staining of young control, old control, and old rmIL-15 intact skin taken during wound surgery after 33 days of treatment and quantification. n = 4-6 mice per group. (G) Flow cytometry analysis of whole blood CD3+/CD8+ cells acquired after 31 days of treatment in uninjured mice. n = 4-6 mice per group. Dashed line denotes epidermis. Data are mean±SEM. *Significantly different ($p < 0.05$) compared to Young PBS. $^{\#}$Significantly different ($p < 0.05$) compared to Old PBS. NS, non-significant ($p > 0.05$).

Figure S3. Recombinant IL-15 therapy in young mice augments wound healing and alters STAT3 signaling. (A) Representative images of wound healing progress and (B) quantification of wound closure over time in control (Young PBS) and rmIL-15 treated (Young rmIL-15) young mice. Dashed white line indicates wound margin. Scale bar = 5 mm. (C) Final wound closure at time of sacrifice on day 9 expressed as a proportion of the original wound area. (D) Wound closure rate per day determined by the average slope of best fit lines. (E) Projected time for full wound closure based on wound closure rate calculated in (D). n = 8-11 mice per group for A-E data. (F) Representative images of $pSTAT3^{Y705}$ immunofluorescent staining in intact skin collected during wound surgery and (G) quantification in the indicated treatment groups. (H) Representative immunofluorescent images of $pSTAT3^{S727}$ staining of intact skin collected during wound surgery and (I) quantification. n = 3 mice per group. Dashed line denotes epidermis. Data are mean±SEM. *Significantly different ($p < 0.05$) relative to Young PBS.

Figure S4. Neutralization of IL-15 in exercising mice prevents the rescue of cellular senescence in aged skin. (A) Representative images of epidermal and dermal HMGB1 and Lamin B1 immunofluorescent staining of young control (Young SED), old control (Old SED) and old rmIL-15 (Old rmIL-15) treated intact skin after 33 days of treatment. (B) Quantification of HMGB1 and (C) Lamin B1 images from (A). n = 3-6 mice per group. (D) Epidermal mRNA expression of the senescence markers p21 (Cdkn1a) and p16ink4a in each treatment group as a fold of young control mice. n = 5-7 mice per group. Dashed line denotes epidermis. Data are mean±SEM; *Significantly different ($p < 0.05$) versus Young SED mice. $^{\#}$Significantly different ($p < 0.05$) relative to Old SED mice. $^{\varphi}$Significantly different ($p < 0.05$) compared to Old EX mice. NS, non-significant ($p > 0.05$).

A

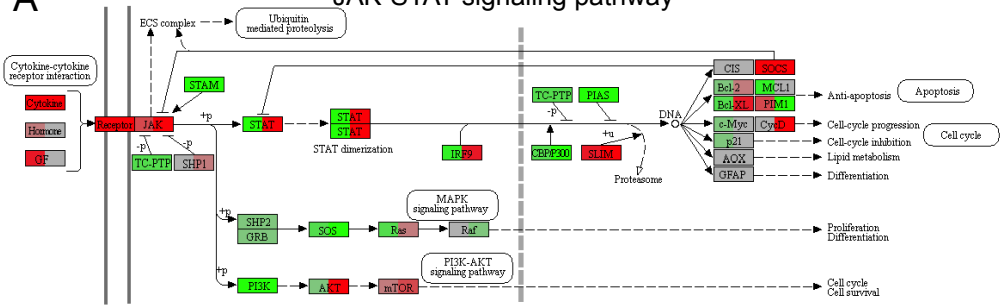
JAK-STAT signaling pathway
ECS complex
Ubiquitin mediated proteolysis
Cytokine-cytokine receptor interaction
Cytokine
Hormone
GF
Receptor
JAK
STAM
STAT
STAT dimerization
IRF9
TC-PTP
SHP1
TC-PTP
PIAS
CBP/P300
SLIM
Proteasome
DNA
CIS
SOCS
Bcl-2
MCL1
Bcl-XL
PIM1
Anti-apoptosis
Apoptosis
c-Myc
CyclD
Cell-cycle progression
Cell-cycle inhibition
Cell cycle
p21
Lipid metabolism
AOX
GFAP
Differentiation
MAPK signaling pathway
SHP2
GRB
SOS
Ras
Raf
Proliferation Differentiation
PI3K-AKT signaling pathway
PI3K
AKT
mTOR
Cell cycle Cell survival

B

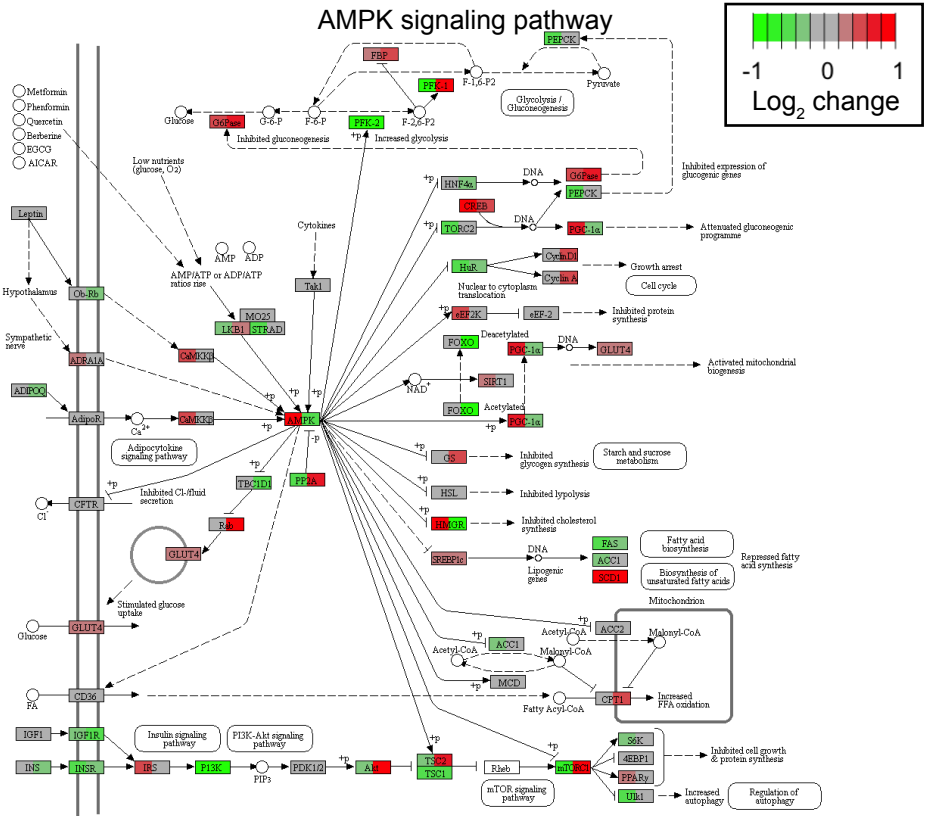
AMPK signaling pathway
-1
0
1
Log2 change
Metformin
Phenformin
Quercetin
Berberine
EGCG
AICAR
Low nutrients (glucose, O2)
AMP
ADP
AMP/ATP or ADP/ATP ratios rise
Leptin
Hypothalamus
Ob-Rb
Sympathetic nerve
ADRA1A
ADIPOQ
AdipoR
Ca2+
CaMKKβ
LKB1
STRAD
MO25
Cytokines
Tak1
AMPK
Adipocytokine signaling pathway
Inhibited Cl-/fluid secretion
CFTR
Cl
TBC1D1
PP2A
Rab
GLUT4
Stimulated glucose uptake
Glucose
GLUT4
FA
CD36
IGF1
IGF1R
INS
INSR
Insulin signaling pathway
IRS
PI3K
PI3K-Akt signaling pathway
PIP3
PDK1/2
Akt
TSC2
TSC1
Rheb
mTORC1
mTOR signaling pathway
S6K
4EBP1
PPARγ
Ulk1
Inhibited cell growth & protein synthesis
Increased autophagy
Regulation of autophagy
FBP
PFKFB1
F-1,6-P2
Glycolysis / Gluconeogenesis
Pyruvate
PEPCK
Glucose
G6Pase
G-6-P
F-6-P
PFK-2
F-2,6-P2
Inhibited gluconeogenesis
Increased glycolysis
HNF4α
CREB
TORC2
DNA
G6Pase
PEPCK
PGC-1α
Inhibited expression of glucogenic genes
Attenuated gluconeogenic programme
HuR
CyclinD1
Cyclin A
Growth arrest
Cell cycle
Nuclear to cytoplasm translocation
eEF2K
eEF-2
Inhibited protein synthesis
FOXO
Deacetylated
PGC-1α
GLUT4
Activated mitochondrial biogenesis
NAD+
SIRT1
FOXO
Acetylated
PGC-1α
GS
Inhibited glycogen synthesis
Starch and sucrose metabolism
HSL
Inhibited lypolysis
HMGR
Inhibited cholesterol synthesis
SREBP1c
DNA
Lipogenic genes
FAS
ACC1
SCD1
Fatty acid biosynthesis
Biosynthesis of unsaturated fatty acids
Repressed fatty acid synthesis
Mitochondrion
Acetyl-CoA
ACC2
Malonyl-CoA
Acetyl-CoA
ACC1
Malonyl-CoA
MCD
Fatty Acyl-CoA
CPT1
Increased FFA oxidation

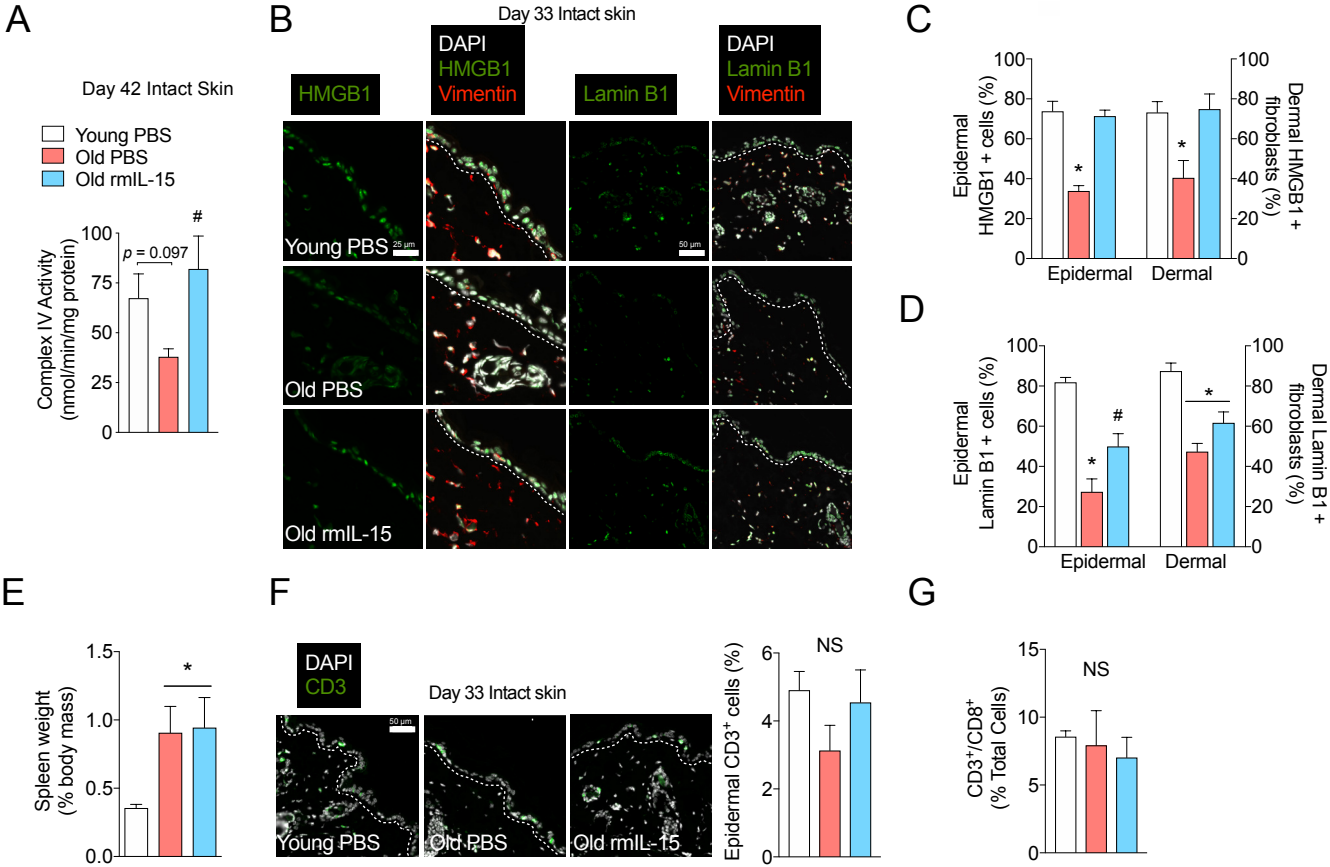
A
Day 42 Intact Skin
Young PBS
Old PBS
Old rmIL-15
Complex IV Activity (nmol/min/mg protein)
p = 0.097
#
B
Day 33 Intact skin
HMGB1
DAPI HMGB1 Vimentin
Lamin B1
DAPI Lamin B1 Vimentin
Young PBS
Old PBS
Old rmIL-15
C
Epidermal HMGB1 + cells (%)
Dermal HMGB1 + fibroblasts (%)
Epidermal
Dermal
D
Epidermal Lamin B1 + cells (%)
Dermal Lamin B1 + fibroblasts (%)
E
Spleen weight (% body mass)
F
DAPI CD3
Day 33 Intact skin
Epidermal CD3+ cells (%)
NS
G
CD3+/CD8+ (% Total Cells)
NS

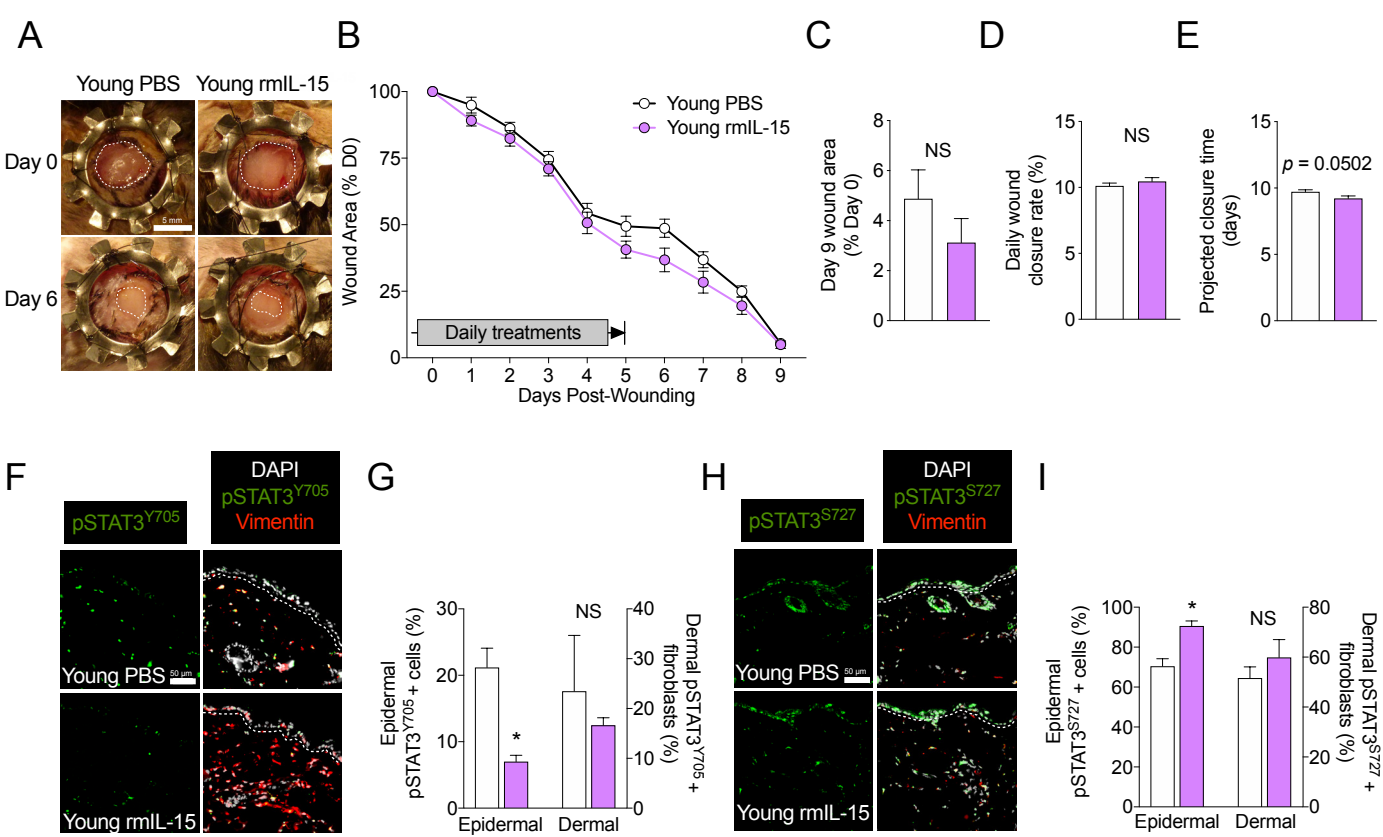
A
Young PBS
Young rmIL-15
Day 0
Day 6
5 mm
B
Wound Area (% D0)
Young PBS
Young rmIL-15
Daily treatments
Days Post-Wounding
C
Day 9 wound area (% Day 0)
NS
D
Daily wound closure rate (%)
NS
E
Projected closure time (days)
p = 0.0502
F
pSTAT3Y705
DAPI
pSTAT3Y705
Vimentin
Young PBS
Young rmIL-15
50 μm
G
Epidermal pSTAT3Y705 + cells (%)
Dermal pSTAT3Y705 + fibroblasts (%)
NS
*
Epidermal
Dermal
H
pSTAT3S727
DAPI
pSTAT3S727
Vimentin
Young PBS
Young rmIL-15
50 μm
I
Epidermal pSTAT3S727 + cells (%)
Dermal pSTAT3S727 + fibroblasts (%)
*
NS
Epidermal
Dermal

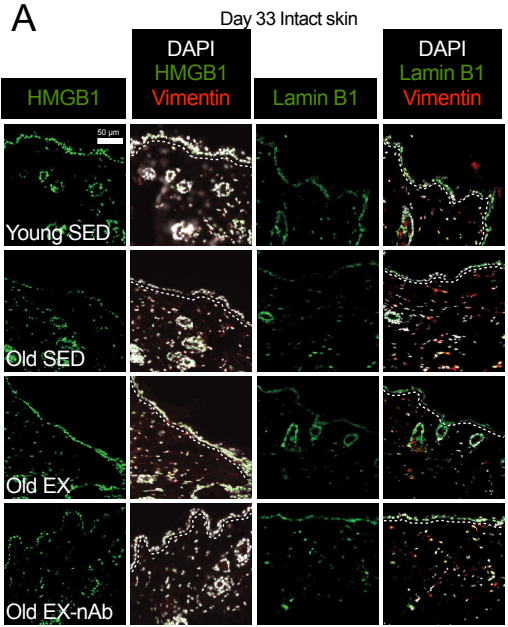
A
Day 33 Intact skin
HMGB1
DAPI
HMGB1
Vimentin
Lamin B1
DAPI
Lamin B1
Vimentin
50 μm
Young SED
Old SED
Old EX
Old EX-nAb

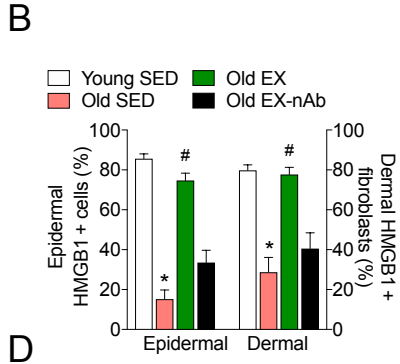
B
Young SED
Old SED
Old EX
Old EX-nAb
Epidermal HMGB1 + cells (%)
Dermal HMGB1 + fibroblasts (%)
Epidermal
Dermal
*
#

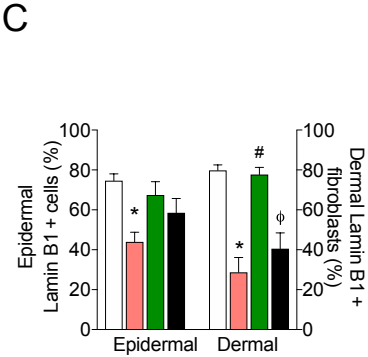
C
Epidermal Lamin B1 + cells (%)
Dermal Lamin B1 + fibroblasts (%)
Epidermal
Dermal
*
#
Φ

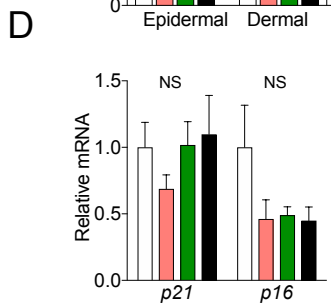
D
Relative mRNA
NS
NS
p21
p16